บรรณานุกรม

[1] T. Bongkarn, G. Rujijanagul. (2006). **Curr Appl. Phys.**, 6, pp. 203.

[2] G. Rujijanagul, N. Vittayakorn, T. Bongkarn. (2007). **Ferroelectric**, 355, pp.84.

[3] G. Rujijanagul, A. Rittidech and T. Bongkarn. (2006). **Mater. Sci. Eng.** A, 438-440. pp. 360-363

[4] Uchino, K. (1996). **Piezoelectric actyators/Utrasonic motors.** London: Kluwer Acadermic Publishers.

[5] J.S. Wringht, L.F. Francis, (1993). **J. Mater. Res.** 8, 1712.

[6] X. Xing, J. Deng, Z. Zhu, G. Lui, (2003). **J. Alloy. Compd.** 353, 1.

[7] Haertling, G.H. (1999). **J. Am. Ceram. Soc.** (82) : 797.

[8] Moulson, A. J. and. Herbert, (2003). J. M. , **Electro ceramics**, second edition,.

[9] Safari, A., Panda, R.K. and Janas, V.F.(1996). **Key. Eng. Mater.** (122) : 35.

[10] Comyn, T. Ph.D. Thesis, (1998). Department of Matrrials, University of Leeds, U. K.

[11] Bongkarn, T. (2005). Ph. D. Thesis, Chiang Mai University, Chiang Mai.

[12] A. J. Moulson and J. M. Herbert. (2003). **Electroceramics**.

[13] G. H. Haretling. (1999). **J. Am. Ceram**. Soc., 82, 797.

[14] http://mylesson.swu.ac.th/ine221/untitled2/lesson2-35.htm

[15] http://th.wikipedia.org/wiki/

[16] บัญชา ธนบุญสมบัติ." การแทรกสอดและการเลี้ยวเบนของคลื่นเบื้องต้น " (2544).ใน การศึกษาวัสดุโดยเทคนิคดิฟแฟรกชัน. หน้า 19 – 26. กรุงเทพฯ : สมาคมส่งเสริมวิทยาศาสตร์และเทคโนโลยี

[17] Cullity,B. C., (1956). X – ray diffraction, Addison – Wesley Publishing Company, USA.

[18] ปราณี รัตนวลีดิโรจน์. " การหาความหนาแน่นด้วยเครื่องชั่งไฟฟ้า (2543). ". เครื่องมือวิจัยทางวัสดุศาสตร์ : ทฤษฎีและการทำงานเบื้องต้น. กรุงเทพฯ : สำนักพิมพ์จุฬาลงกรณ์ มหาวิทยาลัย.

[19] อุดมศักดิ์ อุดมกิจเดชา และคณะ. เครื่องมือวิจัยทางวัสดุศาสตร์: ทฤษฎีและหลักการทำงานเบื้องต้น. กรุงเทพฯ: จุฬาลงกรณ์มหาวิทยาลัย.

[20] Zhi Yu, Chen Ang, Ruyan Guo, A. S. Bhalla, (2002). **Appl. Phys. Lett.**, 81, pp. 7.

[21] Udomporn, A. (2004). Ph. D. Thesis, Chiang Mai University, Chaing Mai.

[22] ดร. สุกานดา เจียรศิริสมบูรณ์, เอกสารประกอบการเรียนการสอนรายวิชา ว. วศ. 210443 (กระบวนการประดิษฐ์สำหรับเซรามิกขั้นสูง), ภาควิชาฟิสิกส์ คณะวิทยาศาสตร์ มหาวิทยาลัยเชียงใหม่.

[23] Udomporn, A. and Ananta, S. (2004). **Curr. Appl. Phys.** (4) : 186 – 185.

[24] Powders Diffraction File no. 35-0739. (2003). n.p. : International Centre for Diffraction Data, Newton Square, PA.

[25] Powders Diffraction File no. 06-0452. (2003). n.p. : International Centre for Diffraction Data, Newton Square, PA.

Output ที่ได้จากโครงการ

List of Publications

1. Perapong Panya, Somnuk Ramaneepikool and *Theerachai Bongkarn* "Dependence of Firing Temperatures on Phase Formation, Microstructure and Phase Transition of $(Pb_{1-x}Ba_x)TiO_3$ Ceramics" Ferroelectrics, 403 (2010) 204-212.
2. Atthakorn Thongtha, Chakkaphan Wattanawikkam and *Theerachai Bongkarn* "Phase Formation and Dielectric Properties of $(Pb_{0.925}Ba_{0.075})(Zr_{1-x}Ti_x)O_3$ Ceramics Prepared by the Solid State Reaction Method" Phase Transitions. (*In press*)

ภาคผนวก

Ferroelectrics, 403:204–212, 2010

ISSN: 0015-0193 print / 1563-5112 online
DOI: 10.1080/00150191003757734

Taylor & Francis
Taylor & Francis Group

Dependence of Firing Temperatures on Phase Formation, Microstructure and Phase Transition of $(Pb_{1-x}Ba_x)TiO_3$ Ceramics

PERAPONG PANYA, SOMNUK RAMANEEPIKOOL, AND THEERACHAI BONGKARN*

Department of Physics, Faculty of Science, Naresuan University, Phitsanulok 65000, Thailand

$(Pb_{1-x}Ba_x)TiO_3$ or PBT ($0.025 \leq x \leq 0.100$) ceramics were prepared via the solid state reaction method. The powders, calcined above 800°C, belonged to a pure tetragonal structure. The c/a ratio of the PBT powders decreased while the average particle size increased with the increasing of calcination temperatures. At the same calcination temperature, the average particle size increased when the Ba ion contents increased. A pure tetragonal structure was found in all PBT ceramics. The densest was discovered in the sample sintered at 1150°C in all compositions. The Curie temperature slightly decreased when the amount of Ba ions increased. The phase transition and dielectric constant were also measured.

Keywords Solid state reaction; tetragonality; calcination temperature; Curie temperature

Introduction

$PbTiO_3$ (PT) is one of the most interesting and most studied perovskites possessing a ferroelectric phase under ambient conditions. The strong interest in this material is caused by its high spontaneous polarization and the wide temperature stability of the ferroelectric phase. PT is used in the field of pyroelectric infrared detectors because of its large pyroelectric coefficient and low permittivity and is also a good material for sensors and actuators [1]. Unfortunately, pure PT, because of its high *c/a* ratio, has been difficult to synthesize as a mechanically robust, high density and monolithic ceramic [2]. However, the dense PT ceramics can be prepared by the substitution of a small amount of dopant, such as isovalent (Ca^{2+}, Ba^{2+}, Sr^{2+}, etc.) or off-valent (Sm^{3+}, Gd^{3+}, Nd^{3+}, etc.) ions into the Pb^{2+} sites. The lattice anisotropy will be decreased and the samples become hard and dense [3–5].

The $(Pb_{1-x}Ba_x)TiO_3$ (PBT) ceramics were prepared by the substitution with small amounts of Ba ions into the Pb ion site. The substitution of Ba^{2+} for Pb^{2+} increases the lattice parameter *a* while decreasing the lattice parameter *c*. The cell parameters continuously, but nonlinearly, change with *x*. [2, 6]. The addition of a Ba ion not only reduced the lattice anisotropy but also maintained the excellent dielectric and piezoelectric anisotropy properties of the PBT ceramics, making it suitable for non-volatile random access memory

Received August 23, 2009; in final form October 17, 2009.
*Corresponding author. E-mail: researchcmu@yahoo.com

(NVRAM) and surface acoustic wave (SAW) [7, 8]. The PBT ceramics can be synthesized by several methods and has been widely reported [9, 10]. Yang and Haile [9] prepared PBT via a sol-gel process. A high purity of $(Pb_{0.5}Ba_{0.5})TiO_3$ powder was obtained at 500°C with a nano-meteric size about 30–50 nm and a specific surface area of 21.91 m^2/g. The particle size of the PBT powders fabricated via the polymeric citrate precursor route were found and ranged between 50 and 54 nm, in all compositions [10].

However, the effects of the addition of small amounts of Ba ions in PT on the phase and morphology evolutions have not been reported yet. Furthermore, the result of firing conditions on phase formation and the microstructure of $(Pb_{1-x}Ba_x)TiO_3$ ceramics are not clearly understood. Therefore, in this present study, the $(Pb_{1-x}Ba_x)TiO_3$ ($0.025 \leq x \leq 0.100$) ceramics were fabricated by the solid state reaction method. The structural phase and microstructure of the samples were studied as a function of firing conditions. In addition, the DSC result and phase transition were also investigated.

Experimental

$(Pb_{1-x}Ba_x)TiO_3$ or PBT ($0.025 \leq x \leq 0.100$) ceramics were prepared by the solid-state reaction method. The starting materials (PbO, $BaCO_3$ and TiO_2) were weighed, mixed and

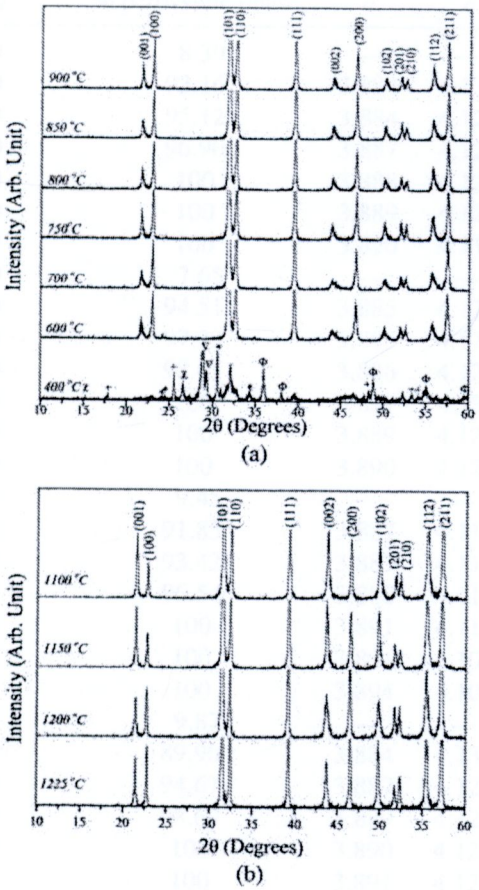

Figure 1. XRD patterns of PBT25; (a) powders calcined at various temperatures and (b) ceramics sintered at different temperatures: (X) TiO, (+) TiO_2, (*) $BaCo_3$, (∇) PbO_2 and (Φ) PbO.

ball-milled for 24 h by the zirconia media in ethyl alcohol. After being dried, the powders were ground in an agate mortar. The mixed powders were calcined at different temperatures (400–900°C) for 4 h in a covered alumina crucible. The PBT calcined powders were pressed into the pellets with a diameter of 15 mm. The pellets were then sintered at temperatures ranging from 1100–1225°C for 2 h. The phase identification of the calcined powders and sintered ceramics were carried out through an X-ray diffractometer. The microstructures were investigated via a scanning electron microscope (SEM). The density of the sintered pellets was measured using the Archimedes method. Silver electrodes were coated on both sides of the polished samples. The room temperature dielectric constant was then measured

Table 1
The percent perovskite phase, lattice parameter *a*, *c*, *c/a* ratio and particle size of PBT powders

Ba^{2+} contents (%)	Calcination temperatures (°C)	% perovskite phase	Lattice parameter (Å)		*c/a* ratio	Average particle size (μm)
			a	*c*		
2.5	400	8.39	—	—	—	0.13
	600	93.16	3.884	4.132	1.064	0.16
	700	95.12	3.884	4.128	1.063	0.24
	750	96.90	3.887	4.127	1.062	0.30
	800	100	3.888	4.124	1.061	0.39
	850	100	3.889	4.121	1.060	0.43
	900	100	3.890	4.114	1.058	0.62
5.0	400	7.65	—	—	—	0.14
	600	94.51	3.885	4.128	1.063	0.19
	700	97.33	3.886	4.125	1.062	0.24
	750	98.65	3.886	4.124	1.061	0.32
	800	100	3.887	4.123	1.061	0.43
	850	100	3.889	4.121	1.060	0.60
	900	100	3.890	4.120	1.059	0.77
7.5	400	9.45	—	—	—	0.14
	600	91.85	3.887	4.115	1.059	0.20
	700	93.42	3.887	4.114	1.058	0.25
	750	96.54	3.888	4.111	1.057	0.33
	800	100	3.891	4.110	1.056	0.44
	850	100	3.891	4.108	1.056	0.59
	900	100	3.894	4.108	1.055	0.65
10.0	400	9.87	—	—	—	0.14
	600	89.90	3.884	4.132	1.064	0.21
	700	94.67	3.887	4.129	1.062	0.25
	750	98.69	3.889	4.126	1.060	0.34
	800	100	3.890	4.122	1.060	0.45
	850	100	3.891	4.120	1.059	0.56
	900	100	3.893	4.117	1.058	0.74

by a LCR meter. The Curie temperature (T_c) of PBT ceramics was evaluated using a differential scanning calorimeter (DSC).

Results and Discussion

Figure 1(a) shows the XRD patterns of $(Pb_{0.975}Ba_{0.025})TiO_3$ (PBT25) powders with different synthesis conditions. The X-ray analysis indicated that the PBT25 powders, calcined from 600 to 900°C, have mainly set peaks with a major peak at (101). All of them belong to the tetragonal phase of a perovskite-type structure and matched with JCPDS file number 06–0452 [11]. For PBT powders calcined below 800°C, impurity phases such as PbO, $BaCO_3$, TiO_2, PbO_2, and TiO were formed. Above 800°C of calcination temperature, the impurity phases disappeared and the pure tetragonal phase was discovered in all samples. The XRD results of $(Pb_{0.950}Ba_{0.050})TiO_3$ (PBT50), $(Pb_{0.925}Ba_{0.075})TiO_3$ (PBT75) and $(Pb_{0.900}Ba_{0.100})TiO_3$ (PBT100) were similar with PBT25.

The relative amounts of the perovskite phase were calculated by measuring the major XRD peak intensities of the perovskite phase. The percentage of perovskite phase is described by the following equation:

$$\% \text{ perovskite phase} = \left(\frac{I_{perov}}{I_{perov} + I_{PbO} + I_{BaCO_3} + I_{TiO_2} + I_{PbO_2} + I_{TiO}} \right) \times 100$$

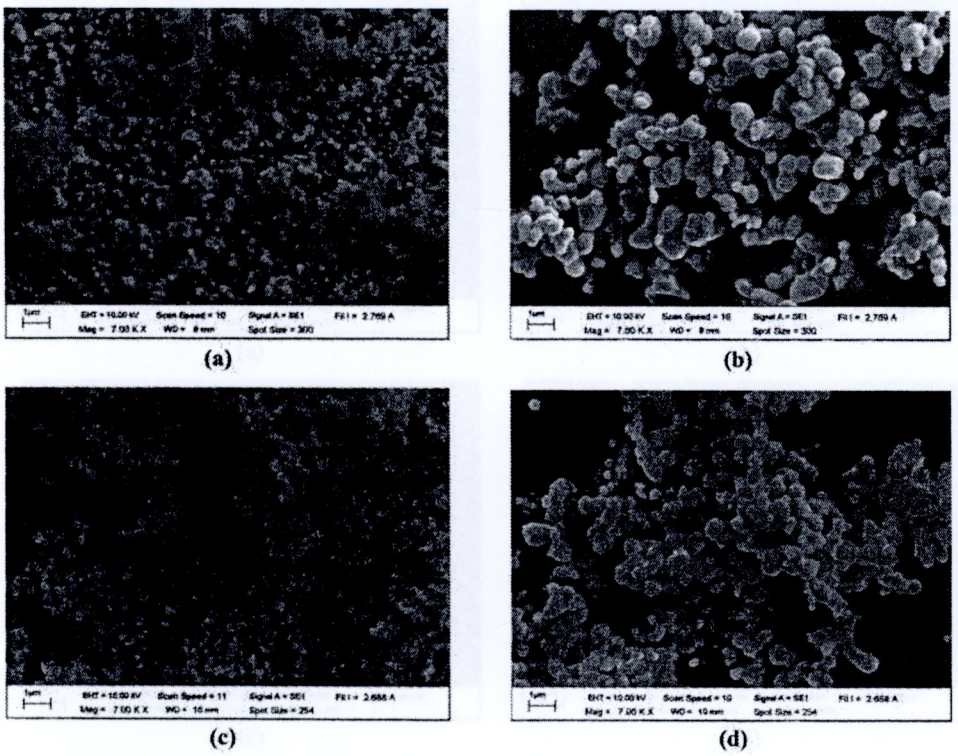

Figure 2. SEM micrographs of the PBT powders: (a) PBT50 calcined at 600°C, (b) PBT50 calcined at 900°C, (c) PBT100 calcined at 600°C and (d) PBT100 calcined at 900°C.

This equation is a well-known equation widely employed in connection with the preparation of complex perovskite structure materials [12, 13]. Where I_{perov}, I_{PbO}, I_{BaCO_3}, I_{TiO_2}, I_{PbO_2} and I_{TiO} refer to the intensity of the (101) perovskite peak, and the intensities of the highest PbO, $BaCO_3$, TiO_2, PbO_2 and TiO, respectively. The percent perovskite phase of PBT powders in all compositions at various calcination temperatures are shown in Table 1. There was an increase in the phase purity with increasing calcination temperatures.

The lattice parameters and tetragonality (*c/a*) of the PBT powders in all compounds at different temperatures (600–900°C) were computed from the (100), (001), (200) and (002) reflective peaks of the XRD patterns and are listed in Table 1. The lattice parameter *c* and *c/a* ratio decreased while the lattice parameter *a* increased with the increasing of the calcination temperatures.

The powders calcined at 800°C were pressed into pellets and sintered from 1100 to 1225°C. Figure 1(b) demonstrates the XRD patterns of the PBT25 sintered pellets at various sintering temperatures. The single tetragonal perovskite phase of PBT was obtained in all compositions. This result was similar with the XRD results of PBT50, PBT75 and PBT100 and indicated that Ba forms a complete solid solution with $(Pb_{1-x}Ba_x)TiO_3$ in the studied composition range. The *c/a* ratio tended to slightly decrease with the increase of Ba ion contents. There is a decrease in the tetragonality of the PBT sample, compared to the PT, due to the incorporation of a smaller Ba ion in the place of the Pb ion site.

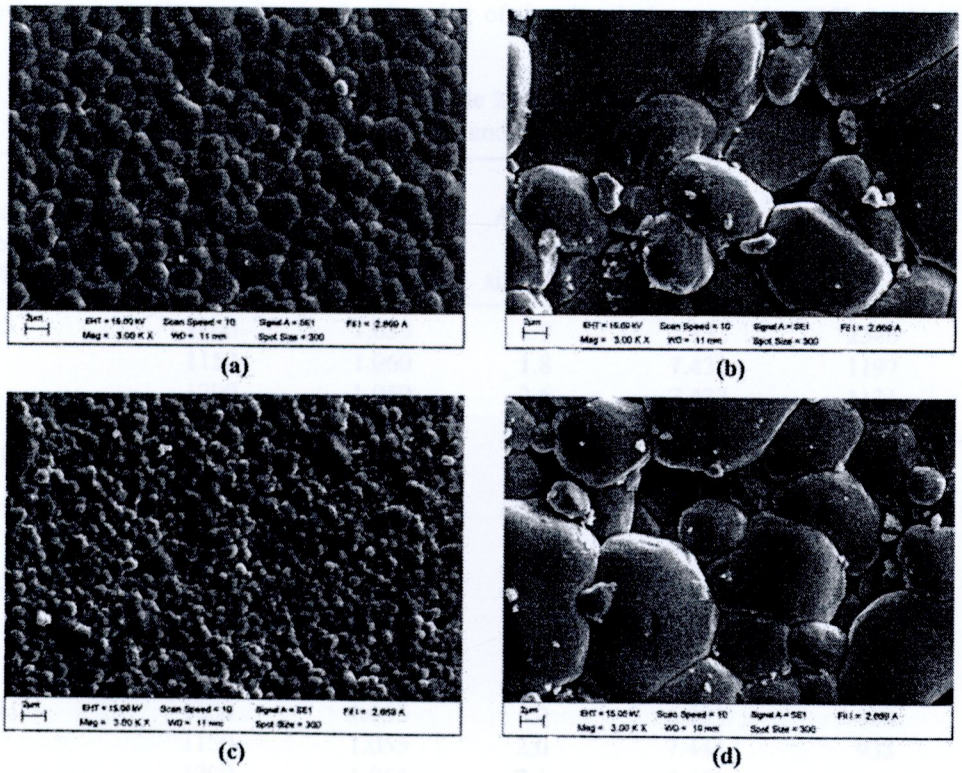

Figure 3. SEM micrographs of the PBT ceramics: (a) PBT25 sintered at 1100°C, (b) PBT25 sintered at 1225°C, (c) PBT75 sintered at 1100°C and (d) PBT75 sintered at 1225°C.

Figure 2 shows the SEM morphology of synthesized PBT powders with different temperatures for 4 h. The synthesized PBT powders consisted of ultra-fine particulates. The particles were highly agglomerated and basically irregular in shape, with a substantial variation in particle size. The powders sintered above 800°C seemed to display a significant level of necking and bonding as if they were in the initial stages of sintering. The obtained particle size of PBT powders increased as the calcination temperatures increased (Table 1). Figure 3 demonstrates the SEM micrographs of PBT ceramics sintered at various temperatures. The grain size tended to increase when the sintering temperatures increased (Table 2).

The densest of the PBT ceramics, in all compounds, were obtained in ceramics sintered at 1150°C as shown in Table 2. The density of the samples increased up to a maximum value of 7.438, 7.310, 7.419 and 7.444 g/cm^3 in samples with $x = 0.025$, 0.050, 0.075 and 0.100, respectively; then the value decreased with the increase in the sintering temperature. The density decreased when the temperature was higher than the optimal temperature. This is because there is a compromise between grain growth and the densification mechanisms during heat treatment, especially during the final stage of sintering. If the sintering rate is too fast and/or if the temperature is too high, the grain growth mechanism is faster than the densification [14].

The tendency of the room temperature dielectric constant decreased, while the grain size tends to increased with the increasing of the sintering temperatures as seen in Table 2. Similar results were reported in $BaTiO_3$, modified $PbTiO_3$, $Pb_{0.9}La_{0.1}TiO_3$ and $Pb(Zr_{0.52}Ti_{0.48})O_3$ ceramics [15–18]. Kakegawa *et al.* described the decrease of the dielectric constant may due to the changing of the chemical composition [18]. In this

Table 2
The *c/a* ratio, average grain size, density and dielectric constant of PBT ceramics

Ba^{2+} contents (%)	Sintering temperatures (°C)	*c/a* ratio	Average grain size (μm)	Density (g/cm^3)	dielectric constant at room temperature
2.5	1100	1.059	1.9	7.132	2348
	1150	1.060	1.8	7.438	1197
	1200	1.059	2.6	7.432	1131
	1225	1.059	5.1	7.412	708
5.0	1100	1.057	1.5	7.282	3151
	1150	1.057	2.0	7.310	1394
	1200	1.057	2.1	7.296	1077
	1225	1.058	8.4	7.235	866
7.5	1100	1.057	0.9	7.343	2550
	1150	1.056	3.0	7.419	1922
	1200	1.057	6.4	7.417	1432
	1225	1.056	5.7	7.412	912
10.0	1100	1.055	1.0	6.983	944
	1150	1.055	2.0	7.444	938
	1200	1.056	7.1	7.405	876
	1225	1.056	4.9	7.280	294

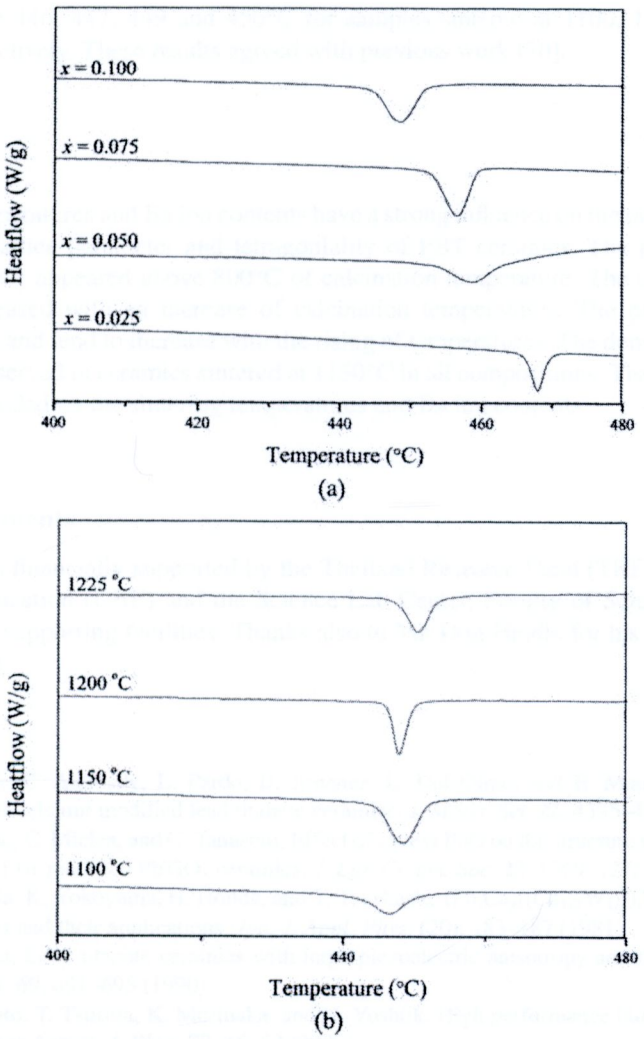

Figure 4. The DSC traces of: (a) PBT pellets sintered at 1150°C with various x and (b) PBT100 pellets with different sintering temperatures.

study, the higher sintering temperature led a greater lead loss, which evaporated above 800°C [19].

The ceramics which were sintered at 1150°C and PBT100 ceramics with different sintering temperatures were selected to study phase transition by DSC measurement. Figure 4(a) shows the DSC graph of PBT ceramics with different x. The endothermic peak associated with the Curie temperature (T_c)—the transition temperature from ferroelectric (FE) to paraelectric (PE) phase—were observed. The T_c was decreased with an increase of Ba ion content. The T_c of PBT ceramics were found to be 468, 459, 457 and 447°C for samples with $x = 0.025$, 0.050, 0.075 and 0.100, respectively. The DSC patterns of PBT100 ceramics with different temperatures are demonstrated in Fig. 4(b). The T_c tended to slightly increase with an increase of sintering temperatures. The T_c of PBT100

ceramics were 446, 447, 449 and 450°C for samples sintered at 1100, 1150, 1200 and 1250°C, respectively. These results agreed with previous work [20].

Conclusions

The firing temperatures and Ba ion contents have a strong influence on the phase formation, morphology, lattice parameter and tetragonlality of PBT ceramics. The pure tetragonal perovskite phase appeared above 800°C of calcination temperature. The tetragonality of powders decreased with an increase of calcination temperatures. The particles have a spherical form and tend to increase with the rising of temperatures. The densest of the PBT pellets was observed in ceramics sintered at 1150°C in all compositions. The T_c of the PBT ceramics depended on the sintering temperatures and Ba ion contents.

Acknowledgments

This work was financially supported by the Thailand Research Fund (TRF), Commission on Higher Education (CHE) and the Science Lab Center, Faculty of Science, Naresuan University for supporting facilities. Thanks also to Mr. Don Hindle for his help in editing the manuscript.

References

1. J. Mendiola, C. Alemany, L. Pardo, B. Jimenez, L. Del Olmo, and E. Maurer, Ferropìezo-electricity of calcium modified lead titanate ceramics. *J. Mater. Sci.* **22**, 4395–4397 (2005).
2. L. Amarande, C. Miclea, and C. Tanasoiu, Effect of excess PbO on the structure and piezoelectric properties of Bi-modified $PbTiO_3$ ceramics. *J. Eur. Ceram. Soc.* **22**, 1269–1275 (2002).
3. Y. Yamashita, K. Yokoyama, H. Honda, and T. Takahashi, (Pb,Ca)[$(Co_{1/2}W_{1/2})$,Ti]O_3 piezoelectric ceramics and their applications. *Jpn. J. Appl. Phys.* (20): 183–187 (1981).
4. T. Takahashi, Lead titanate ceramics with large piezoelectric anisotropy and their application. *Ceram. Bull.* **69**, 691–695 (1990).
5. K. Hashimoto, T. Tsuruta, K. Morinaka, and N. Yoshiik, High performance human information sensor. *Sensor Actuat. A-Phys.* **79**, 46–52 (2000).
6. X. Xing, J. Deng, Z. Zhu, and G. Lui, Solid solution Ba_{1-x} Pb_x TiO_3 and its thermal expansion. *J. Alloy. Comp.* **353**, 1–4 (2003).
7. A. M. Glazer and S. A. Mabud, Powder profile refinement of lead zirconate titanate at several temperatures. II. Pure $PbTiO_3$. *Acta Crystallogr. B.* **B34**, 1065–1070 (1978).
8. G. Shirane, R. Pepinsky, and B. C. Frazer, X-ray and neutron diffraction study of ferroelectric $PbTiO_2$. *Acta Crystallogr.* **9**, 131–140 (1956).
9. W. D. Yang and S. M. Haile, Characterization and microstructure of highly preferred oriented lead barium titanate thin films on MgO (100) by sol-gel process. *Thin Solid Films.* **510**, 55–51 (2006).
10. P. R. Arya, P. Jha, G. N. Subbanna, and A. K. Ganguli, Polymeric citrate precursor route to the synthesis of nano-sized barium lead titanates. *Mater. Res. Bull.* **38**, 617–628 (2003).
11. Powder Diffraction File No. 06-0452: International Center for Diffraction Data. Newton Square: PA; 2003.
12. R. Sumang and T. Bongkarn, The effect of calcination temperatures on the phase formation and microstructure of $(Pb_{1-x}Sr_x)TiO_3$ powders. *Key Eng. Mater.* **421–422**, 243–246 (2010).
13. T. Bongkarn and W. Tangkawsakul, Low temperature preparation of antiferroelectric PZ and PBZ powders using the combustion technique. *Ferroelectrics* **383**, 50–56 (2009).

14. B. Guillaume, F. Boschini, L. Garcia-Cano, A. Rulmont, R. Cloots, and M. Ausloos, Optimization of $BaZrO_3$ sintering by control of the initial powder size distribution; a factorial design statistical analysis. *J. Eur. Ceram. Soc.* **25**, 3593–3604 (2005).
15. K. Kinoshita and A. Yamaji, Grain-size effects on dielectric properties in barium titanate ceramics. *J. Appl. Phys.* **47**, 371–373 (1976).
16. T. Y. Chen, S. Y. Chu, and Y. D. Juang, Effects of sintering temperature on the dielectric and piezoelectric properties of Sr additive Sm-modified $PbTiO_3$ ceramics. *Sensor. Actuat. A-Phys.* **102**, 6–10 (2002).
17. B. S. Kang, D. G. Choi, and S. K. Choi, Effect of grain size on pyroelectric and dielectric properties of $Pb_{0.9}La_{0.1}TiO_3$ ceramics. *J. Mater. Sci.* **9**, 139–144 (1998).
18. K. Kakegawa, J. Mohri, T. Takahashi, H. Yamamura, and S. Shirasaki, A compositional fluctuation and properties of $Pb(Zr,Ti)O_3$. *Solid State Commun.* **24**, 769–772 (1977).
19. B. P. Pokharel and D. Pandey, Dielectric studies of phase transitions in $(Pb_{1-x}Ba_x)ZrO_3$. *J. Appl. Phys.* **88**, 5364–5374 (2000).
20. M. T. Hossain, S. Islam, M. H. Mondal, and A. H. Khan, Studies on anomalous behaviour at Curie point, T_c of some glasses of mixed ferrites. *Bangladesh J. Sci. Ind. Res.* **41**(3–4), 171–180 (2006).

Phase Transitions
2011, 1–8, iFirst

Taylor & Francis
Taylor & Francis Group

Phase formation and dielectric properties of $(Pb_{0.925}Ba_{0.075})(Zr_{1-x}Ti_x)O_3$ ceramics prepared by the solid-state reaction method

Atthakorn Thongtha, Chakkaphan Wattanawikkam and Theerachai Bongkarn*

Department of Physics, Faculty of Science, Naresuan University, Phitsanulok 65000, Thailand

(*Received 11 December 2010; final version received 21 June 2011*)

Lead barium zirconate titanate $[(Pb_{0.925}Ba_{0.075})(Zr_{1-x}Ti_x)O_3]$ ceramics with $0 \leq x \leq 1$ were prepared by the solid-state reaction method. The calcination temperatures were between 800°C and 1000°C for 1 h and the sintering temperature was 1200°C for 3 h. It was found that the structure of the calcined powders and sintered pellets was in an orthorhombic phase for $x = 0$; a rhombohedral phase for $x = 0.25$ and a tetragonal phase for $0.5 \leq x \leq 1$. The c/a ratio increased with an increase in the x content. The average particle size and density slightly decreased with an increase in the x content, while the average grain size, linear shrinkage, and Curie temperature increased when the x content increased.

Keywords: lead barium zirconate titanate; microstructure; phase transition; crystal structure; dielectric properties

1. Introduction

Lead barium zirconate $(Pb_{1-x}Ba_x)ZrO_3$ (PBZ) is one of the perovskite structure materials discovered by Roberts [1,2] in 1950. The investigation of the structural phase at room temperature indicated that: PBZ with $0 \leq x \leq 0.175$ has an orthorhombic anti-ferroelectric phase; PBZ with $0.175 < x \leq 0.35$ has a rhombohedral ferroelectric phase; and PBZ with $0.35 < x \leq 1$ has a cubic paraelectric phase [3–6]. The Curie temperature of the PBZ materials decreased with the increase of x, from 230°C for $x = 0$ to 50°C for $x = 0.35$ [7]. The maximum dielectric constant at Curie temperature was observed at $x = 0.25$ and a relaxor ferroelectric behavior was exhibited at $x = 0.30$ [7]. For $x \leq 0.10$, the electric field induced an anti-ferroelectric-to-ferroelectric phase transition which gave a large increase in volume [3,8,9]. Specifically, the anti-ferroelectric-to-ferroelectric phase transition of $(Pb_{0.925}Ba_{0.075})ZrO_3$ ceramics exhibited high expansion, which makes this ceramic an interesting candidate for application in large-displacement actuator devices [3].

Lead barium titanate $(Pb_{1-x}Ba_x)TiO_3$ (PBT) with $0 \leq x \leq 1$ is a perovskite ferroelectric material which has a tetragonal structure at room temperature [10–14]. It changes from a ferroelectric to a paraelectric phase when it receives a certain Curie temperature. The Curie temperature of PBT materials drops monotonically with an increase of x, from 490°C at

*Corresponding author. Email: researchcmu@yahoo.com

ISSN 0141-1594 print/ISSN 1029-0338 online

DOI: 10.1080/01411594.2011.599563
http://www.informaworld.com

$x = 0$ to 120°C at $x = 1$ [15]. $(Pb_{0.925}Ba_{0.075})TiO_3$ has a high Curie temperature (~457°C) [13,14]. It has been considered for use in high-temperature electric and optical devices.

Lead barium zirconate titanate (PBZT) ceramic is a solid system composed of orthorhombic anti-ferroelectric, rhombohedral ferroelectric, cubic paraelectric PBZ, and ferroelectric PBT. Recently, Ujma et al. [16–18] studied the dielectric properties of $(Pb_{0.75}Ba_{0.25})(Zr_{0.70}Ti_{0.30})O_3$ ceramic which is the solid solution of rhombohedral ferroelectric PBZ and tetragonal ferroelectric PBT. They found typical relaxor behavior. The magnitude of the dielectric constant decreased and the maximum shifted to higher temperatures with increased frequency. After a survey of the literature, it was found that the dielectric properties and phase transition of a solid solution of orthorhombic anti-ferroelectric PBZ and tetragonal ferroelectric PBT have not been studied. Therefore, in this study, the phase formation, microstructure, phase transition, and dielectric properties of $(Pb_{0.925}Ba_{0.075})(Zr_{1-x}Ti_x)O_3$ (PBZT) ceramics with $0 \leq x \leq 1$ were investigated. The PBZT ceramics were prepared by the solid-state reaction method. The structural phase, microstructure, dielectric constant, and dielectric loss with a variation of frequencies of the PBZT ceramics were characterized by a X-ray diffractometer (XRD), scanning electron microscopy (SEM), and LCR meter.

2. Experimental

The $(Pb_{0.925}Ba_{0.075})(Zr_{1-x}Ti_x)O_3$ ceramics with $0 \leq x \leq 1$ were prepared by a conventional solid-state reaction method. The raw materials of PbO, $BaCO_3$, ZrO_2, and TiO_2 were weighed and mixed by ball milling in ethanol using zirconia balls for 24 h. After drying and sieving, they were calcined between 800°C and 1000°C for 1 h. The calcined powders were reground by ball milling and mixed with 2 wt% binder for 24 h. The calcined powders were then dried, crushed, and sieved. The powders were isostatically pressed at 80 MPa into 15 mm diameter pellets. Finally, the pellets were sintered at 1200°C for 3 h. In order to minimize the loss of lead due to vaporization, the PbO atmosphere during the sintering process was maintained using lead titanate and lead zirconate as the spacer powders. The crystal structure and microstructure of the calcined and sintered samples were characterized by an XRD and SEM, respectively. The average particle size and average grain size were determined using a mean linear intercept method. The Archimedes displacement method with distilled water was employed to evaluate the sample's density. Silver paste was coated and fired at 550°C for 5 min to form electrodes. Dielectric constants with various frequencies were also measured by an LCR meter.

3. Results and discussion

Figure 1 shows the XRD pattern of PBZT powders with $0 \leq x \leq 1$. The pure perovskite phase was observed for all compositions. For $x = 0$, the structural phase, indexed in an orthorhombic phase, matched the JCPDS file number 35-0739 [19] and corresponded to previous works [3,5,7,20]. For $x = 0.25$, the structural phase belonged to the rhombohedral phase which matched the JCPDS file number 29-0775 [21]. For $0.5 \leq x \leq 1$, the samples indexed in the tetragonal phase matched JCPDS file number 06-0452 [22], as shown in Figure 1(a). To investigate the range of the rhombohedral structure, the XRD patterns of $x = 0.05$, 0.1, 0.2, 0.3, 0.4, and 0.45 were also studied, as shown in Figure 1(b). The structural phase changed from orthorhombic to rhombohedral and rhombohedral to tetragonal when $x = 0.05$ and 0.4, respectively. The XRD results from the sintered pellets

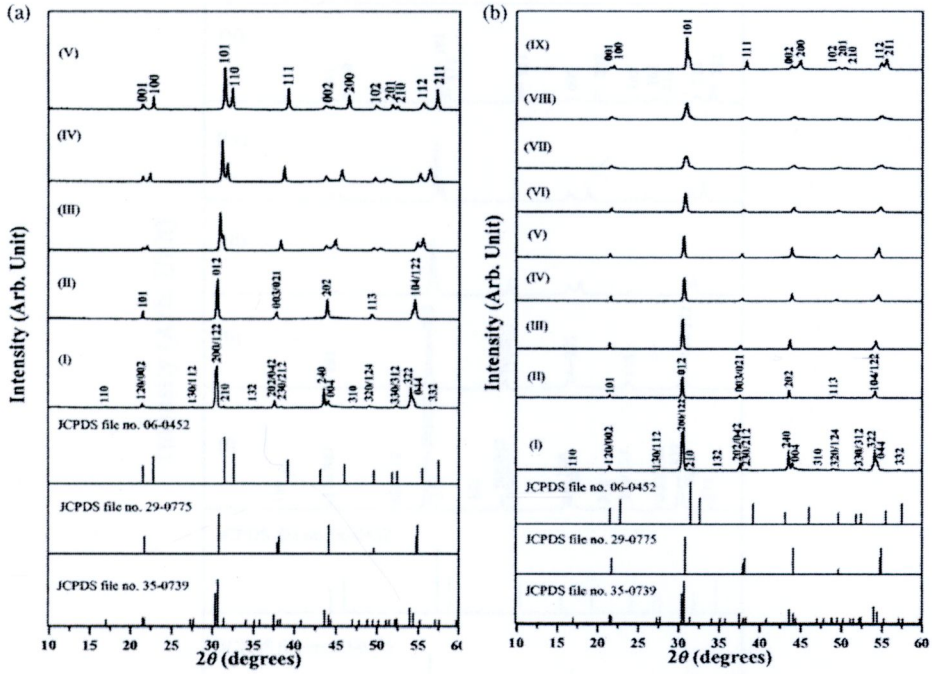

Figure 1. (a) XRD pattern of PBZT powders with (I) $x = 0$ calcined at 1000°C, (II) $x = 0.25$ calcined at 950°C, (III) $x = 0.5$ calcined at 900°C, (IV) $x = 0.75$ calcined at 850°C, and (V) $x = 1$ calcined at 800°C. (b) XRD pattern of PBZT powders with (I) $x = 0$ calcined at 1000°C, (II) $x = 0.05$ calcined at 990°C, (III) $x = 0.1$ calcined at 980°C, (IV) $x = 0.2$ calcined at 960°C, (V) $x = 0.25$ calcined at 950°C, (VI) $x = 0.3$ calcined at 940°C, (VII) $x = 0.4$ calcined at 920°C, (VIII) $x = 0.45$ calcined at 910°C, and (IX) $x = 0.5$ calcined at 900°C.

were similar to the results from the XRD powders, as shown in Figure 2. The lattice parameters a, b, and c of the PBZT ceramics were calculated by the least square method and are shown in Table 1. For $0.5 \leq x \leq 1$, the lattice parameters a and c decreased with increased x values. The c/a ratio increased while the unit cell volume decreased when the x values increased, as given in Table 1.

The SEM morphology of the PBZT powders is shown in Figure 3(a)–(c). The particles were agglomerated and were irregular in shape with a variation in particle size. The average particle size of $0 \leq x \leq 0.75$ showed little difference in their values, while the value in the size of the $x = 1$ sample rapidly decreased. The average particle size of $0 \leq x \leq 1$ was between 0.4 and 1.7 μm. The change of the PBZT ceramic surface morphology was a function of increasing x, as shown in Figure 3(d)–(f). The increase of the average grain sizes was between 2.3 and 3.9 μm when the x content was increased from 0 to 1, as given in Table 1. The measured density and linear shrinkage with the variation of the x content are shown in Table 1. The increase of the x content also affected density and linear shrinkage. The density tended to decrease, while the linear shrinkage tended to increase with the increase of x. The obtained density of all samples was around 96% of the theoretical density.

Figure 4(a)–(c) illustrates the temperature dependence of the dielectric constant (ε_r) of PBZT ceramics at various frequencies. For $x = 0$, the dielectric constant showed two peaks. The first peak showed an anomaly around 105°C, which was due to the phase

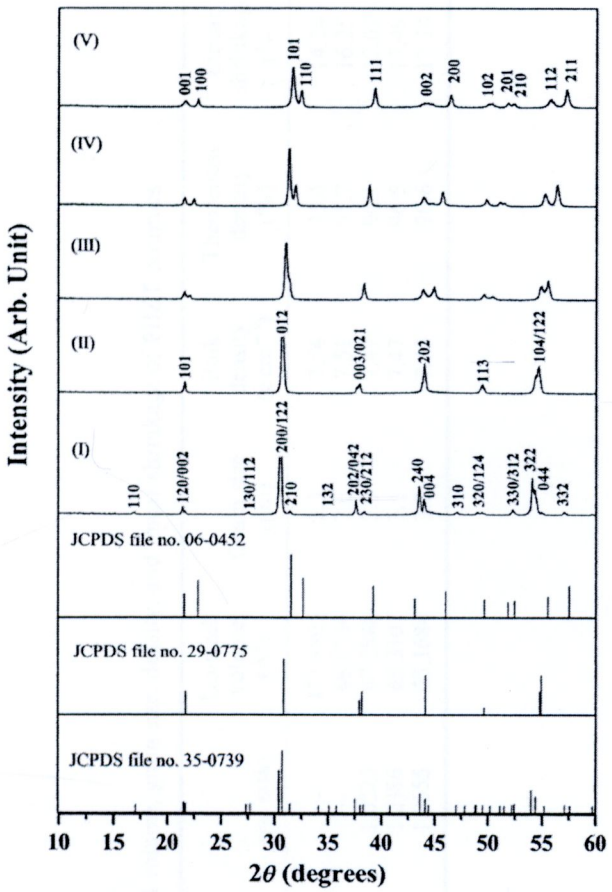

Figure 2. XRD pattern of PBZT ceramics sintered at 1200°C with: (I) $x=0$, (II) $x=0.25$, (III) $x=0.5$, (IV) $x=0.75$, and (V) $x=1$.

transition from an antiferroelectric to a ferroelectric state. This phase transition was explained and confirmed by previous works [3,6,7,9]. The second peak was at around 202°C, which was caused by a ferroelectric–paraelectric transformation process, as shown in Figure 4(a). When the content of x increased, the anomalous peak vanished but the ferroelectric–paraelectric phase transition still occurred and the Curie temperature moved toward a higher temperature, as shown in Figure 4(a)–(d). At varied frequencies, the samples with $x=0$ did not change the Curie temperature, as is demonstrated in Figure 4(a), while $x \geq 0.25$ effected the shift of Curie temperature, as shown in Figure 4(b) and (c) and is listed in Table 2. The Curie temperature shifted to a higher temperature with increased frequency. The dielectric constant at a Curie temperature of $x \geq 0.25$ decreased when the frequency increased from 1 to 100 kHz, as shown in Figure 4(b) and (c). This is a typical behavior of relaxor ferroelectrics with $x \geq 0.25$. For $x \geq 0.25$, the result is similar to previous works describing $(Pb_{0.75}Ba_{0.25})(Zr_{0.70}Ti_{0.30})O_3$ ceramics [16–18]. For the same frequency at 1, 10, and 100 kHz, the dielectric constant at room temperature first increased and reached its highest at $x=0.75$ and then the value dropped when x was higher than 0.75, as given in Table 2. The frequency and content of x affected the dielectric properties.

Table 1. Crystal structure, lattice parameters, c/a ratio, unit cell volume, grain size, density, and linear shrinkage of PBZT ceramics.

X	Crystal structure	Lattice parameters (Å)			c/a ratio	Unit cell volume ($Å^3$)	Grain size (μm)	Bulk density ($g\,cm^{-3}$)	Theoretical density (%)	Linear shrinkage (%)
		a	b	c						
0	Orthorhombic	5.2459	11.4839	7.8661	–	473.8805	2.3	7.54	95.4	14.24
0.25	Rhombohedral	4.1188	4.1188	4.1188	–	69.8734	2.6	7.51	95.7	16.25
0.5	Tetragonal	4.0426	4.0426	4.1355	1.0225	67.5848	3.0	7.49	96.1	17.09
0.75	Tetragonal	3.9766	3.9766	4.1301	1.0386	65.3107	3.1	7.47	96.5	17.49
1	Tetragonal	3.9115	3.9115	4.1287	1.0555	63.1684	3.9	7.43	96.6	17.74

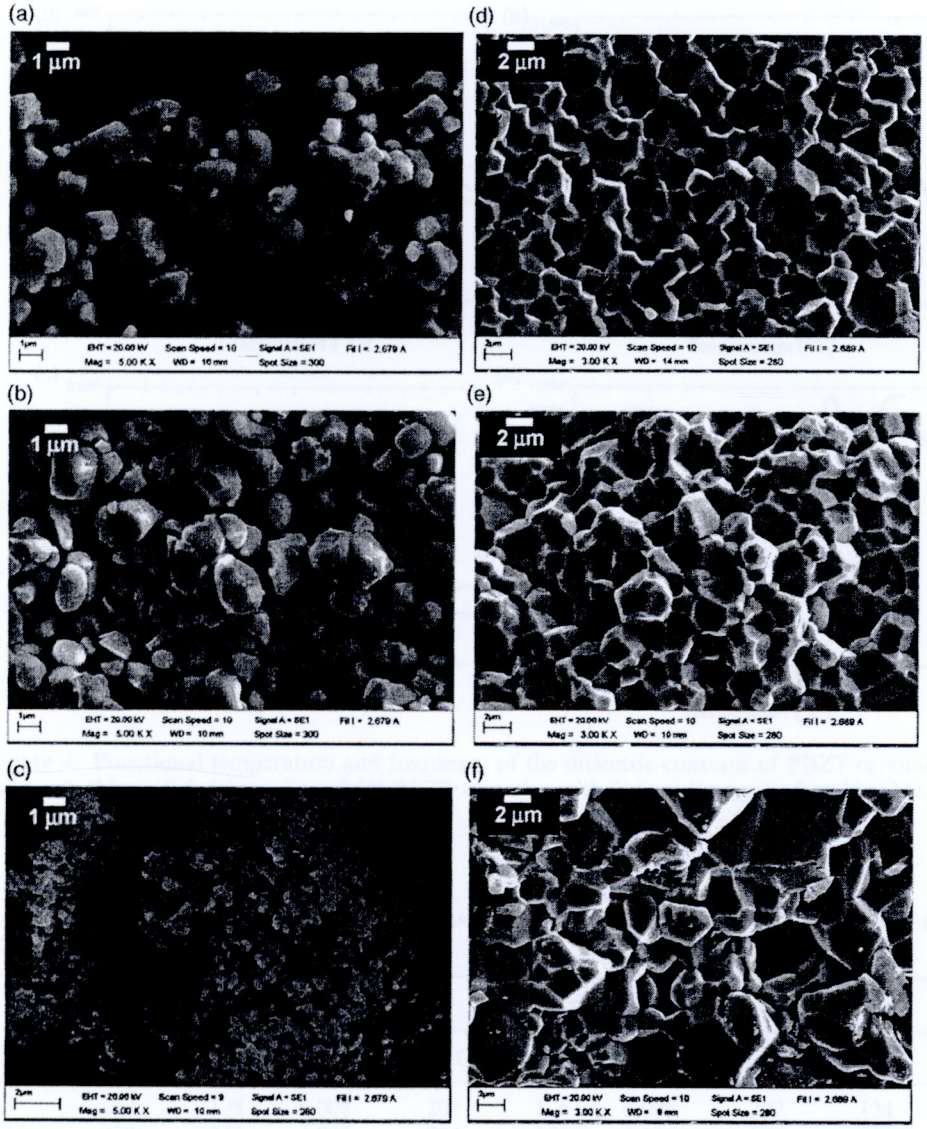

Figure 3. SEM morphology of PBZT powders with: (a) $x = 0.5$ calcined at 900°C, (b) $x = 0.75$ calcined at 850°C, and (c) $x = 1$ calcined at 800°C and PBZT ceramics with: (d) $x = 0.5$, (e) $x = 0.75$, and (f) $x = 1$ sintered at 1200°C.

4. Conclusions

The results indicated that the concentration of Zr^{4+} and Ti^{4+} ions has a significant effect on the phase formation, microstructure, and dielectric properties of PBZT ceramics. The structure phase of $(Pb_{0.925}Ba_{0.075})(Zr_{1-x}Ti_x)O_3$ (PBZT) samples is in an orthorhombic phase for $x = 0$; a rhombohedral phase for $x = 0.25$ and a tetragonal phase for $0.5 \leq x \leq 1$. The average particle is 0.4–1.7 μm and the average grain size is 2.3–3.9 μm. The linear shrinkage, average grain size, and Curie temperature of the PBZT increased, while the

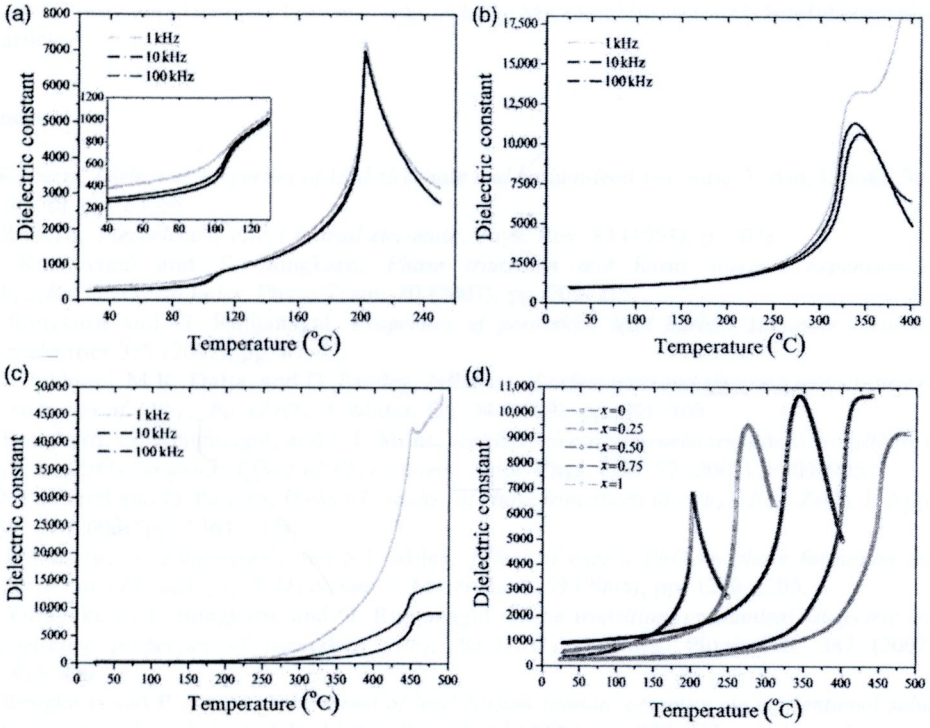

Figure 4. Functional temperature and frequency of the dielectric constant of PBZT ceramics with: (a) $x=0$, (b) $x=0.5$, (c) $x=1$, and (d) PBZT ceramics with $0 \leq x \leq 1$ measured at 100 kHz.

Table 2. Curie temperature (T_c), dielectric constant (ε_r), and loss tangent ($\tan\delta$) of PBZT ceramic at room temperature.

	1 kHz			10 kHz			100 kHz		
x	T_c (°C)	ε_r	$\tan\delta$	T_c (°C)	ε_r	$\tan\delta$	T_c (°C)	ε_r	$\tan\delta$
0	202	128	0.008	202	126	0.006	202	124	0.005
0.25	272	253	0.032	274	251	0.006	274	250	0.002
0.5	337	878	0.002	338	875	0.002	344	873	0.002
0.75	405	920	0.003	407	917	0.002	410	915	0.002
1	450	268	0.084	452	216	0.051	458	204	0.016

average particle size and density decreased, when the x content increased. Typical relaxor ferroelectrics were discovered in the PBZT sample with $x \geq 0.25$.

Acknowledgments

This study was financially supported by Thailand Research Fund (TRF) and Commission in Higher Education (CHE). The authors also thank the Department of Physics, Faculty of Science, Naresuan

University for providing facilities. They also acknowledge Mr. Don Hindle for his helpful correction of this article.

References

[1] S. Roberts, *Dielectric properties of lead zirconate and barium-lead zirconate*, J. Am. Ceram. Soc. 33 (1950), pp. 63–66.
[2] S. Roberts, *Piezoelectric effect in lead zirconate*, Phys. Rev. 83 (1951), p. 1078.
[3] G. Rujijanagul and T. Bongkarn, *Phase transition and linear thermal expansion of* $(Pb_{1-x}Ba_x)ZrO_3$ *ceramics*, Phase Trans. 80 (2007), pp. 209–215.
[4] T. Bongkarn and G. Rujijanagul, *Properties of perovskite lead barium zirconate ceramics*, Ferroelectrics 358 (2007), pp. 67–73.
[5] B.P. Pokharel, M.K. Datta, and D. Pandey, *Influence of calcination and sintering temperature on the structure of* $(Pb_{1-x}Ba_x)ZrO_3$, J. Mater. Sci. 34 (1999), pp. 691–700.
[6] T. Bongkarn, G. Rujijanagul, and S.J. Milne, *Antiferroelectric-ferroelectric phase transitions in* $Pb_{1-x}Ba_xZrO_3$ *ceramics: Effect of PbO content*, Appl. Phys. Lett. 92 (2008), p. 092905.
[7] B.P. Pokharel and D. Pandey, *Dielectric studies of phase transitions in* $(Pb_{1-x}Ba_x)ZrO_3$, J. Appl. Phys. 88 (2000), pp. 5364–5373.
[8] T. Bongkarn, G. Rujijanagul, and S.J. Milne, *Effect of excess PbO on phase formation and properties of* $(Pb_{0.90}Ba_{0.10})ZrO_3$ *ceramics*, Mater. Lett. 59 (2005), pp. 1200–1205.
[9] N. Vittayakorn, T. Bongkarn, and G. Rujijanagul, *Phase transition, mechanical, dielectric and piezoelectric properties of perovskite* $(Pb_{1-x}Ba_x)ZrO_3$ *ceramics*, Physica B. 387 (2007), pp. 415–420.
[10] T. Bongkarn and P. Panya, *Fabrication of lead barium titanate ceramics via conventional solid-state mixed oxide technique*, Adv. Mater. Res. 55–57 (2008), pp. 209–212.
[11] W.D. Yang and S.M. Haile, *Highly preferred oriented lead barium titanate thin films using acetylacetone as chelating agent in sol-gel process*, Rev. Adv. Mater. Sci. 10 (2005), pp. 143–148.
[12] X. Xing, J. Deng, Z. Zhu, and G. Liu, *Solid solution* $Ba_{1-x}Pb_xTiO_3$ *and its thermal expansion*, J. Alloy. Comp. 353 (2003), pp. 1–4.
[13] R. Sumang and T. Bongkarn, *Phase formation, microstructure and phase transition of lead barium titanate ceramics: Effect of PbO content*, Ferroelectrics 383 (2009), pp. 57–64.
[14] P. Panya, S. Ramaneepikool, and T. Bongkarn, *Dependence of firing temperatures on phase formation, microstructure and phase transition of* $(Pb_{1-x}Ba_x)TiO_3$ *ceramics*, Ferroelectrics 403 (2010), pp. 204–212.
[15] O.Z. Yanchevskii, O.I. V'yunov, and A.G. Beloous, *Fabrication and properties of semiconducting barium lead titanate ceramics containing low-melting glass additions*, Inorg. Mater. 39 (2003), pp. 645–651.
[16] Z. Ujma, M. Adamczyk, and J. Handerek, *Relaxor properties of* $(Pb_{0.75}Ba_{0.25})(Zr_{0.70}Ti_{0.30})O_3$ *ceramics*, J. Eur. Ceram. Soc. 18 (1998), pp. 2201–2207.
[17] J. Handerek, M. Adamczyk, and Z. Ujma, *Dielectric and pyroelectric properties of* $(Pb_{0.75}Ba_{0.25})(Zr_{0.70}Ti_{0.30})O_3$ $[x=0.25\div0.35]$ *ceramics exhibiting the relaxor ferroelectrics behaviour*, Ferroelectrics 233 (1999), pp. 253–270.
[18] M. Adamczyk, Z. Ujma, and J. Handerek, *Relaxor behavior of La-modified* $(Pb_{0.75}Ba_{0.25})(Zr_{0.70}Ti_{0.30})O_3$ *ceramics*, J. Appl. Phys. 89 (2001), pp. 542–547.
[19] Powder Diffraction File No. 35-0739, International Centre for Diffraction Data, Newton Square, PA, 2000.
[20] B.P. Pokharel and D. Pandey, *High temperature x-ray diffraction studies on antiferroelectric and ferroelectric phase transitions in* $(Pb_{1-x}Ba_x)ZrO_3$ $(x=0.05,0.10)$, J. Appl. Phys. 90 (2001), pp. 2985–2994.
[21] Powder Diffraction File No. 29-0775, International Centre for Diffraction Data, Newton Square, PA, 2000.
[22] Powder Diffraction File No. 06-0452, International Centre for Diffraction Data, Newton Square, PA, 2000.